The Kinetics and Shape Factors of Ultrafine Dry Grinding in a Laboratory Tumbling Ball Mill

Leonard G. Austin, M. Yekeler, Timothy F. Dumm, Richard Hogg*

Dedicated to Professor Kurt Leschonski on the occasion of his 60th birthday

(Received: 24 September 1990)

Abstract

The kinetics of batch grinding quartz from a feed of 600 by 425 μm to a product of 80% less than 10 μm have been determined using screening and laser diffractometer sizing for size analysis. The specific rates of breakage decreased by a factor of about three when the material became less than about 100 μm in size, but the primary breakage distribution function also changed to give proportionately more fine material, so that the grinding efficiency expressed as the development of surface area (B.E.T.) per unit of energy input did not decrease. Analysis of the shape of the particles in the 25 × 38 μm size range showed that particles of this size produced by roll crushing or by 8 minutes of grinding of a 425 × 600 μm feed were not different but at long grinding times the particles were rounded. This suggests that the breakage mechanism changes to give more chipping and abrasion and less disintegrative fracture. As the material approached the ultrafine size range it adhered to the mill case and there was no further size reduction. However, a technique for striking the mill case to dislodge the particles was successful in allowing further grinding to 40% by weight less than 2 μm.

1 Introduction

It has long been known that it is difficult to accomplish ultrafine grinding in a tumbling ball mill. It has been reported [12, 13] that there is no further size reduction after some hours of grinding cement clinker in laboratory ball mills. *Austin* and *Bagga* [1] and *Shah* and *Austin* [16] have given an analysis of the kinetics of dry grinding in a laboratory ball mill, introducing the concept of a slowing-down factor κ, which is the ratio of the specific rates of breakage at some long time of grinding to the normal specific rates of breakage. They showed that this factor decreased as fine material accumulated in the mill charge. *Cottaar* and co-workers [8–10] showed that the movement of solid in a dry laboratory ball mill was influenced by the fineness of the solid and by the presence of air, and that evacuation of air from the mill caused particle sedimentation and low rates of breakage.

The concept of the slowing-down factor has also been used in wet grinding [17, 18]. At very high slurry concentrations it appears to be correlated with a steady decrease of mill power caused by the build up of a layer of deposit sticking to the mill case. This reduces the effective mill diameter and, eventually, the balls start to adhere in the layer and centrifuge. A decrease of mill power always indicates less lifting and tumbling of the media and, hence, less breakage. However, slowing-down of breakage rates was also observed at lower slurry concentrations where there was no change in mill power.

In this paper we extend the results of these workers to dry grinding of particles to about 80% by weight less than 10 μm in a laboratory tumbling ball mill.

2 Experimental Methods

Dry grinding was carried out in the laboratory ball mill described in Table 1, at a low ball load of 20% of the mill volume filled with the ball bed and a low powder load cor-

Table 1: Ball mill characteristics and test conditions.

Mill	Inner diameter, mm	194
	Length, mm	175
	Volume, cm^3	5170
	Operational speed, rpm	75
	% critical speed	76
	Net mill power, watts	~10
Lifters	Number	6
	Cross-section	semi-circular
	Radius, mm	10
Media (Balls)	Material	alloy steel
	Diameter, mm	25
	Number	74
	Specific gravity	7.8
	Average ball weight, g	66.2
	Fractional mill filling J	0.20
Material	Quartz	
	Specific gravity	2.65
	Powder weight, g	320

* Prof. *L. G. Austin, M. Yekeler, T. F. Dumm,* Prof. *R. Hogg,* Department of Mineral Engineering, The Pennsylvania State University, University Park, PA 16802 (USA).

responding to a formal interstitial filling of the void spaces of the ball bed of $U = 0.5$. These conditions were chosen because it is known [2] that both dry and wet grinding give normal first-order grinding kinetics under these loading conditions. After each grinding period the mill was left long enough to allow the particles to settle, the balls were cleaned and removed from the mill one-by-one and the mixed powder was spoon-sampled to obtain a sample for screen analysis. The balls and screened material were returned to the mill for further grinding after size analysis.

The sample weights were adjusted to give no more than 5 to 10 g of powder less than 400 mesh (38 μm). After dry screening for 20 minutes in a stack of standard sieves on a Rotap sieving machine, the material on the screens was washed under a water spray to remove adherent fine powder before drying and weighing. The washings (smaller than 400 mesh) were collected and filtered in a vacuum filter and the filter material added to the 0 × 400 mesh fraction. The small amounts of weight loss, typically less than 0.5%, were added to the weight of the 0 × 400 mesh fraction weight for calculations of the cumulative size distribution. One gram samples were taken for size analysis by laser diffractometer (Microtrac SRA and SPA models, Leeds and Northrup, Microtrac Division, Largo, FL 33543). Fine iron wear dust was extracted from the quartz ground for long times by using a magnet but the quantities were too small to affect the product size distributions (less than 0.40%).

The material studied was a white crystalline quartz which we have used extensively as a reproducible standard material for grinding studies.

3 Experimental Results

Figure 1 shows the initial grinding results plotted in first-order form [2]:

$$w_1(t) = w_1(0) \exp(-S_1 t), \quad (1)$$

where $w_1(t)$ is the fraction remaining in the feed size interval after time t and S_1 is the specific rate of breakage of that size.

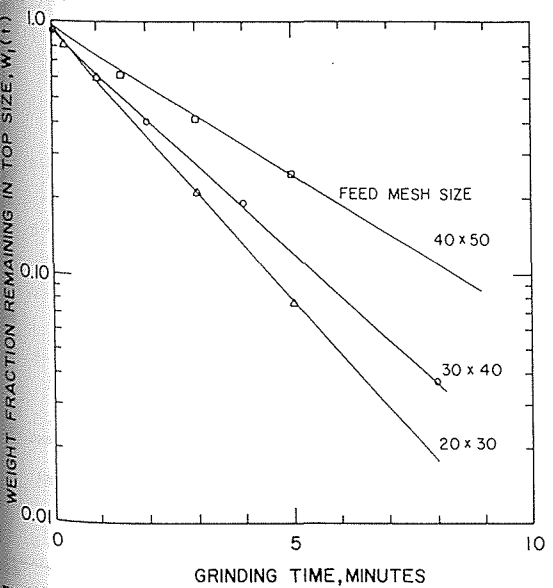

Fig. 1: First order plots of breakage of screened feed of quartz, dry grinding in a laboratory ball mill (D = 194 mm, d = 25 mm, fraction of critical speed = 0.76, J = 0.20, U = 0.5).

As shown in Figure 2, the values of S can be fitted to the expression [2]

$$S_i = a_T (x_i/x_o)^{\alpha} \frac{1}{1 + (x/\mu)^{\Lambda}} \quad (2)$$

with $a_T = 0.6$ min^{-1}, $\alpha = 0.80$, $\mu = 1.9$ mm, $\Lambda = 3.7$ and $x_o = 1$ mm, in agreement with results reported by *Bagga* [7] on the same material under the same conditions.

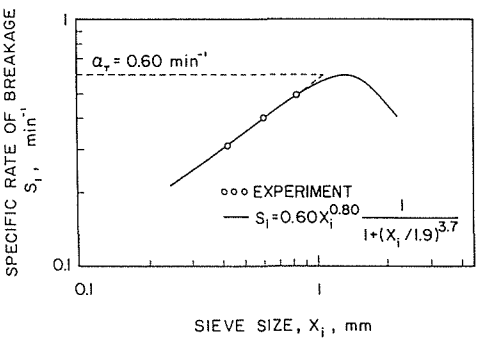

Fig. 2: Variation of first-order specific rates of breakage with particle size: $\sqrt{2}$ intervals, plotted at upper size of interval (see Figure 1).

The cumulative primary breakage distribution function [2] determined using the BII procedure [3] is shown in Figure 3. This fits the expression [2]

$$B_{i,1} = \Phi (x_{i-1}/x_1)^{\gamma} + (1 - \Phi)(x_{i-1}/x_1)^{\beta}, \quad i > 1 \quad (3)$$

where x_i is the top size of the i^{th} $\sqrt{2}$ size interval counted down from $i = 1$ for the 30 × 40 mesh feed. $B_{i,1}$ is the weight fraction of primary breakage products which fall less than x_i.

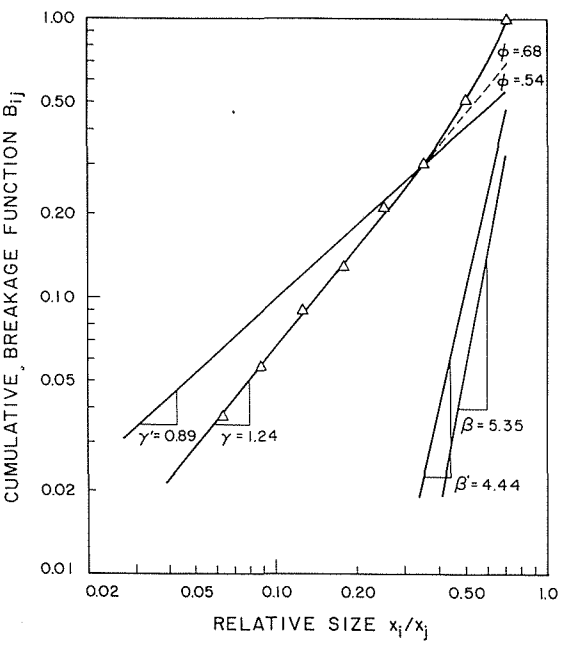

Fig. 3: Primary breakage distribution function of 30 × 40 mesh quartz feed (see Figure 1): – direct measurement from 1 minute grinding data; △ experimental; --- estimated to fit grinding data above 16 minutes;

Figure 4 shows the particle size distributions obtained at various times of grinding. The laser diffractometer size distributions were joined to the sieve size distributions by correcting to

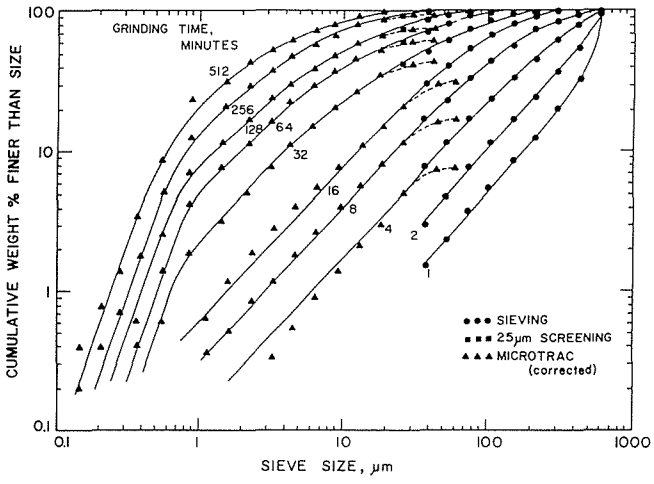

Fig. 4: Product size distributions from dry grinding of 30 × 40 mesh quartz in the laboratory ball mill.

equivalent sieve size [4, 5]. The shape factor defined by $d_{50}/\bar{x}$ was found to be 1.20 for both the SRA and SPA instruments, where d_{50} is the mass median laser diffractometer size and $\bar{x}$ is the geometric mean size of the $\sqrt{2}$ screen interval of the tested material. The SRA instrument was used for grinding times of 16 minutes or less.

For the longer grinding times the material was wet screened on 25 μm sieves (75 mm diameter, *W. S. Tyler* Co., Mentor, OH, 44060) and the minus 25 μm material analyzed in the Microtrac SPA instrument.

It must be remembered that laser diffractometers do not see very small particles, so the small amounts of finer material compared to the extrapolation of the size distributions of larger sizes, which occurs below 1 μm, is probably not real. The variability in the reproducibility of the instrument for repeated analysis is small compared to the changes in the size distributions shown in Figure 4. Table 2 shows the variation of B.E.T. (N_2) specific surface area determined on the fine material, compared to the specific surface area calculated from the size analysis. The large difference between the two areas, with the ratio increasing with the grinding time, is a clear indication that the diffractometer size analysis misses more and more of the finest material as the material becomes smaller at longer grinding times.

Table 2: Specific surface areas of material less than 400 mesh (38 μm).

Grinding time minutes	B.E.T. m^2/g	Microtrac m^2/g	Ratio (B.E.T./Microtrac)
32	0.87	0.41	2.12
64	1.2	0.57	2.11
128	1.9	0.66	2.86
256	3.7	0.96	3.83
512	7.2	1.37	5.28

4 Treatment of Data

In the light of past experience the results of grinding up to 16 minutes of grinding time were simulated using the characteristic parameters of α, μ, Λ, β, γ and Φ in the Penn State Ball Mill Simulator [6]. It was assumed that B values were dimensionally normalized (i.e. Φ constant, irrespective of breaking size), that breakage was first-order and that values of S and B for the small sizes could be obtained from Eqs. (2) and (3) with the same characteristic parameters. The simulation gave good agreement with the experimental data up to 16 minutes of grinding. However, in accordance with past experience, the predicted size distributions at 32 minutes and longer were then finer than those observed experimentally.

This was treated using the false time concept [1, 2, 16], by making the simulator produce a match to a specified point on the product size distribution and designating the grinding time necessary to achieve this match as the false time θ, where $\theta \leq t$. However, it became obvious that another change was also occurring at these longer grinding times. In order to fit the experimental data at grinding times greater than 16 minutes it was necessary to change the B values as indicated in Figure 3, to parameters of $\gamma = 0.90$, $\Phi = 0.55$, $\beta = 4.5$, With these B values it was possible to obtain the correct shape of the product size distributions down to 1 μm.

It was found that even with these changes it was only possible to simulate the data up to 256 minutes of grinding. The product size distribution at 512 minutes was not finer and the powder was found to be caked to the case of the mill. To prevent this effect the mill was mounted inside another cylinder of 380 mm diameter, and 98 balls of 19 mm diameter were placed in the space between the two cylinders. During rotation, the balls in the annulus also tumbled and struck the case of the inner mill, dislodging powder adherent to the case. This eliminated caking on the wall up to 512 minutes, but not at 1024 minutes of grinding. The values given in Figure 4 for the 512 minutes are for grinding in the modified (struck) mill from 256 to 512 minutes. Figure 5 shows the comparison of simulated and experimental values based on choosing a false time to give a one-point fit of the simulated result to an experimental point with between 40 to 50% of material less than the chosen size. The simulation gives reasonable agreement with the experimental data in the range of sizes greater than 1 micrometer.

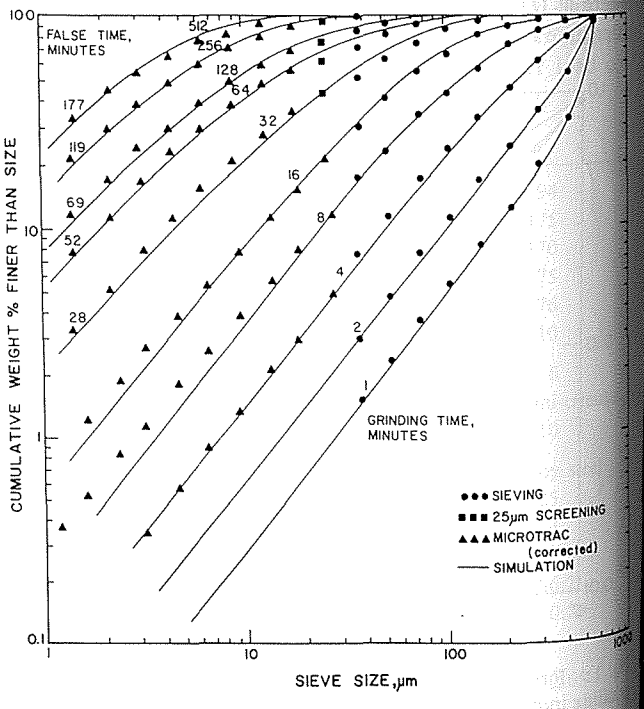

Fig. 5: Simulated and experimental product size distributions.

Figure 6 shows the relation between the false first-order time and the real grinding time. Differentiation of this curve gives the value of the slowing-down factor κ

$$\kappa = d\theta/dt \, . \tag{4}$$

A major change in κ can be seen between about 30 and 60 minutes of grinding.
However, the time of grinding is not the important variable, since it is only an index of the fineness of the size distribution

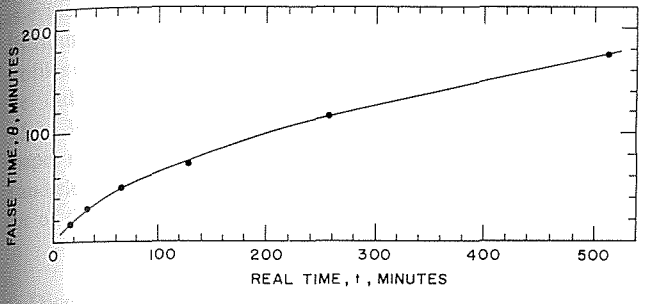

Fig. 6: False time (apparent first-order grinding time) versus real grinding time (see Figure 5).

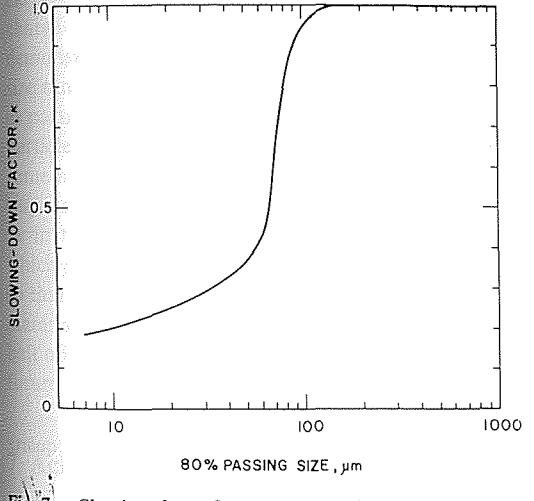

Fig. 7: Slowing-down factor κ versus the 80% passing size in the mill.

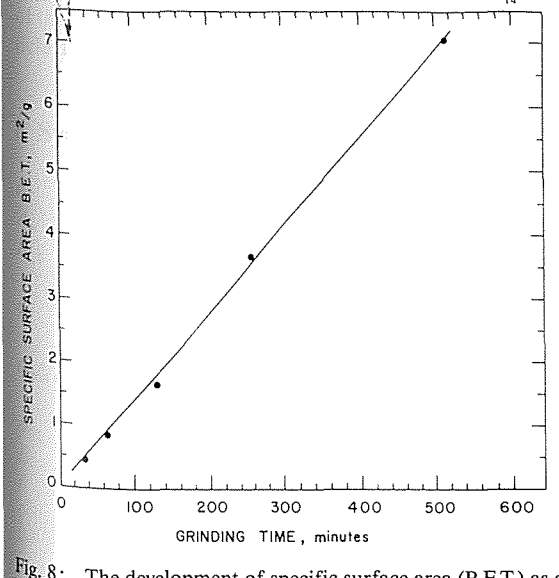

Fig. 8: The development of specific surface area (B.E.T.) as a function of time of grinding.

in the mill. Figure 7 shows κ plotted versus the 80% passing size. The grinding clearly changes its character when the material in the mill is finer than about 100 μm. The specific rates of breakage fall to about one-third of the usual values, and then decrease less abruptly, and the primary breakage distribution becomes flatter (see Figure 3), leading to a bigger proportion of the finest material.
Figure 8 shows the development of BET specific surface area versus grinding time. If the efficiency of grinding is defined in terms of the increase in specific surface area per unit of energy input it appears that the grinding up to 512 minutes (8.5 hours) and a net energy input of about 250 kWh/ton is almost at a constant efficiency. This energy input corresponds to a size distribution of more than 80% less than 10 μm and 25% less than 1 μm.

5 Shape Analysis

Examination of Figure 4 suggests that the laser diffractometer size analysis and the screen analysis do not join consistently at the long grinding times. Examination with a scanning electron microscope showed that the particles produced at the long grinding times were more rounded than the irregular fragments formed at shorter grinding times. The shape factor for spheres would be expected to be 1, so reducing Microtrac size by a factor of 1.2 to convert it to sieve size is an overcorrection at long grinding times.
In order to investigate the change in shape in more detail, an SEM under computer control [11] was used to obtain perimeter coordinates of particles (screened between 25 and 38 μm) lying on a beryllium slide. The particles were first dispersed in a solution of 0.1 weight % sodium metaphosphate, 0.1% Daxad 11 KLS (W. R. Grace CO.) and 0.1% Aerosol-OT (Fisher Scientific Co.) in distilled water, then slides were prepared using a freeze-drying technique [11] which prevents particle reagglomeration. The concentration of particles in the solution was changed until slides were obtained where the particles were not touching but yet had a convenient number density on the slide. After carbon coating in the usual way, about a hundred particles were automatically analyzed for perimeter co-ordinates.
The results were expressed in terms of shape factors developed to indicate the "sharpness" of the particles. The perimeter co-ordinates of a plane image of a particle were used to determine the area, the centroid and the equivalent circular diameter. The vector of perimeter coordinates taken as the beam of the SEM marches round the perameter was reduced by dividing into 20, that is, for 1000 points every 50th point was taken. This is equivalent to representing the perimeter profile by a 20-sided polygon, as shown in Figure 9. The distance R from the centroid to each of these 20 perimeters points was calculated as was the internal angle ϕ and the Feret's diameter d_F. The elongation E for a particle is defined [19] as

$$E = d_{FL}/d_{Fmin} \tag{5}$$

where d_{Fmin} is the smallest value of Feret's diameter and d_{FL} is the Feret's diameter perpendicular to d_{Fmin}.
The mean contained angle for a polygon of n equal sides fitted into a circle is

$$\phi_c = \pi\,(n - 2)/n \, . \tag{6}$$

A contained angle at a point on a polygon fitted into an irregular particle deviates more from a circle as

$|(\phi_c/\phi) - 1| > 0$. Thus *Dumm* [11] defines a mean "angular variability" for a particle by

$$A_v = 1 + \sum_{k=1}^{n} \left(\frac{\phi_c}{\phi_k} - 1 \right)^2 \qquad (7)$$

which is 1 for a circle.

These indices were developed because neither the fractal dimension [14] or the coefficient of particle signature analysis [15] were found to distinguish between particles of obviously different shape.

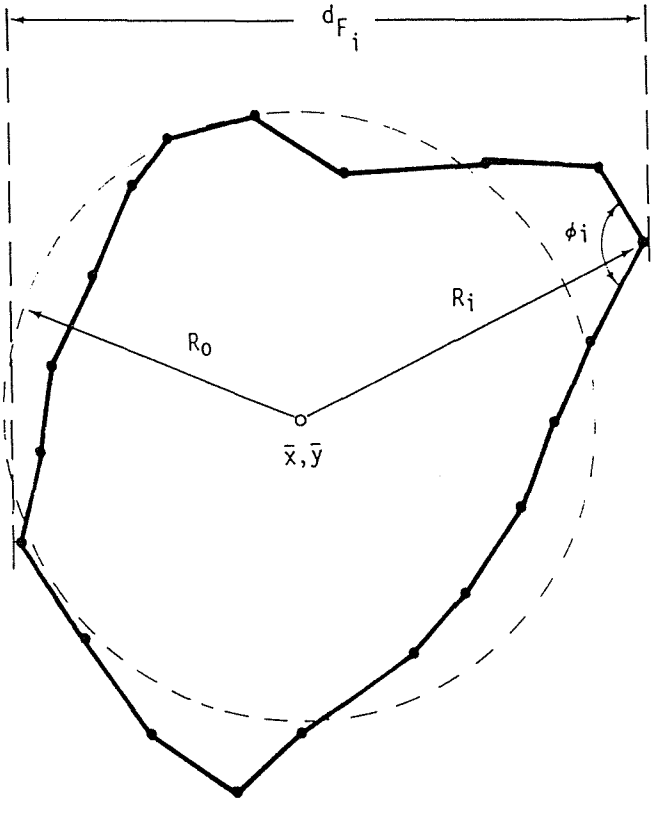

Fig. 9: Plot of a particle profile of 20 points showing the centroid $(\bar{x}, \bar{y})$, the mean radius R_0 and the values of R, ϕ and d_f corresponding to the i^{th} perimeter point.

Figures 10 and 11 show the values of elongation and angular variability determined from 25 × 38 µm material screened from a roll crusher product, (from which the 425 × 600 µm feed to the ball milling was obtained) from the ball mill product after 8 minutes of grinding, and from the product after 256 minutes of grinding, based on analysis of about 100 particles in each case. There is no significant difference in angular variability between the original material and that produced by 8 minutes

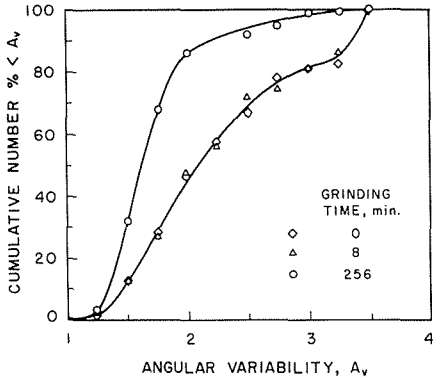

Fig. 10: Cumulative number distributions of angular variability of quartz particles of 25 × 38 µm screen size.

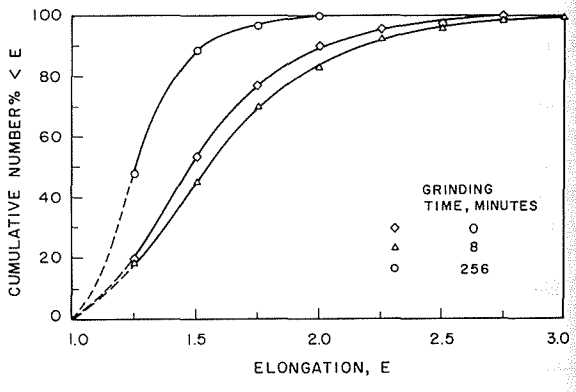

Fig. 11: Cumulative number distributions of elongation of quartz particles of 25 × 38 µm screen size.

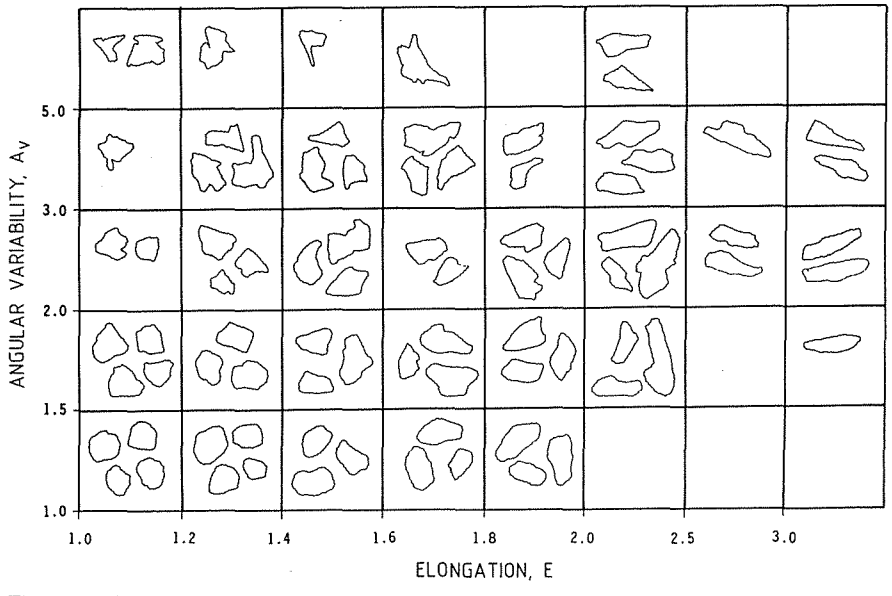

Fig. 12: Plot of quartz particle profiles in angular variability versus elongation scheme showing how the differences in shapes relate to their assigned shape class values.

of grinding, but the 256 minute material is clearly different. The median angularity has decreased from about 2.1 to 1.6 and the percentage of particles with angular variability greater than 3 has decreased from 20% to 1%. Similarly, the median elongation has decreased from about 1.5 to 1.25, the spread has decreased drastically, and particles with elongations greater than 2 have disappeared.

It is concluded that particles are becoming more spherical and that long particles are being removed, at the long grinding times. This correlates with the breakage mechanism changing to give more chipping and abrasion and less disintegrative fracture, as evidenced by the change in shape of the primary breakage distribution function. Figure 12 shows the computer-printed profiles of particles having angular variability and elongation in the indicated ranges. The major percentage of particles (25 × 38 μm) at 256 minutes of grinding correspond to the shapes in the six blocks with angular variability between 1 and 2 and elongation between 1 and 1.6, at the bottom left hand corner of the figure.

6 Discussion and Conclusions

In order to dry ball mill quartz to the ultrafine region of a particle size range of 1 to 10 μm it was necessary to prevent the charge of fine powder from adhering to the case. The work demonstrates the techniques necessary for data analysis for this size range and indicates that the character of grinding changes as particle size becomes less than about 100 μm. The shapes of particles of a given size (25 × 38 μm) present after grinding for some hours were more rounded than those present in the early stages of grinding. The change in breakage character appears to be in the direction of a slower chipping or abrasion process which gives small product fragments and rounded larger sizes, so that the size distributions contain proportionately more fine material. The systematic investigation of the kinetics of fine dry ball milling, and extension to wet grinding, is a project for the future.

7 Acknowledgements

We gratefully acknowledge financial support for this work from Award No. 89A1223 of BP America, Inc., Cleveland, OH. Parts of this paper were presented at the Second World Congress Particle Technology, Kyoto, Japan, September 1990.

8 Symbols and Abbreviations

a_T characteristic constant in Eq. (2), fraction per minute
A_v angular variability defined by Eq. (7)
$B_{i,1}$ cumulative primary breakage function of size 1; fraction broken to less than size x_i in one breakage
d_F Feret's diameter at co-ordinate point on the perimeter of a plane image of a particle
d_{min} minimum Feret's diameter of the plane image of a particle
d_{FL} Feret's diameter perpendicular to d_{Fmin}
E elongation defined by Eq. (5)
i integer denoting $\sqrt{2}$ size interval
J fraction of mill volume filled with ball bed
n the number of sides of a polygon fitted to the perimeter co-ordinates of the microscope plane image of a particle
R distance from the centroid to a perimeter co-ordinate
R_o radius of a circle of the same area as the plane image of a particle
S_i specific rate of breakage of material of size interval i, fraction per minute
t time of grinding, minutes
U fraction of void spaces in ball bed filled with powder
$w_i(t)$ fraction of mill charge in size interval i
x_i size of particles, mm
x_o standard size, 1 mm
$\bar{x}, \bar{y}$ coordinates of the centroid of a plane image of a particle
α characteristic constant in Eq. (2)
β characteristic constant in Eq. (3)
ϕ the angle contained between two adjacent sides of a polygon at a perimeter co-ordinate at the corner
ϕ_c the average contained angle for an n-sided polygon of equal sides fitted into a circle
Φ characteristic constant in Eq. (3)
γ characteristic constant in Eq. (3)
Λ characteristic constant in Eq. (2)
μ characteristic constant in Eq. (2), mm
κ slowing down factor: ratio of specific rate of breakage at time t to normal specific rate of breakage at time zero
θ false time, minutes

9 References

[1] *L. G. Austin, P. Bagga:* Powder Technol. *28* (1981) 83.
[2] *L. G. Austin, R. R. Klimpel, P. T. Luckie:* Process Engineering of Size Reduction: Ball Milling, SME/AIME, Inc., New York, NY, (1984) pp. 586.
[3] *L. G. Austin, P. T. Luckie:* Powder Technol. *5* (1972) 215.
[4] *L. G. Austin, I. Shah:* Powder Technol. *35* (1983) 271.
[5] *L. G. Austin, O. Trass, T. F. Dumm, V. R. Koka:* Part. Part. Syst. Charact. *5* (1988) 13.
[6] *L. G. Austin, K. Yildirim, P. T. Luckie, H. C. Cho:* Two Stage Ball Mill Circuit Simulator PSUSIM, Department of Mineral Engineering, The Pennsylvania State University, University Park, PA 16802 (1989).
[7] *P. Bagga:* The Development of Standard Format for Presenting the Breakage Parameters of Particles in Tumbling Ball Mills, M. S. Thesis, The Pennsylvania State University, University Park, PA 16802 (1979).
[8] *W. Cottaar, A. Heynen, K. Rietema:* Powder Technol. *46* (1986) 219.
[9] *W. Cottaar, K. Rietema:* Powder Technol. *38* (1984) 183.
[10] *W. Cottaar, K. Rietema:* Powder Technol. *43* (1985) 189.
[11] *T. Dumm:* Characterization of Size/Composition and Shape of Fine Coal and Mineral Particles, PhD. Thesis, The Pennsylvania State University, University Park, PA 16802 (1989).
[12] *G. Ghigi, L. Rabottino:* Dechema Monograph. *57* (1967) 427.
[13] *R. T. Hukki, I. G. Reddy:* Dechema Monograph. *57* (1967) 313.
[14] *B. H. Kaye:* Powder Technol. *21* (1978) 1.
[15] *T. P. Meloy, N. Clark:* Proc. 10th Powder and Bulk Solids Conference, Rosemont, IL (1985) 102.
[16] *I. Shah, L. G. Austin:* in: *S. G. Malghan* (ed.): Ultrafine Grinding and Separation of Industrial Minerals, AIME, New York, NY (1983) 9.
[17] *C. Tangsathitkulchai, L. G. Austin:* Powder Technol. *42* (1985) 287.
[18] *C. Tangsathitkulchai, L. G. Austin:* Powder Technol. *59* (1989) 4.
[19] *J. Tsubaki, G. Jimbo:* Powder Technol. *22* (1979) 161.